Results in Engineering 22 (2024) 102107

Contents lists available at ScienceDirect

Results in Engineering

journal homepage: www.sciencedirect.com/journal/results-in-engineering

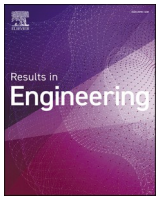

Optimizing long-term park-level integrated energy system through multi-stage planning: A study incorporating the ladder-type carbon trading mechanism

Kaiyue Li [a], Jingyu Ran [a], Moon Keun Kim [b], Zhe Tian [c,d,**], Jiying Liu [a,*]

[a] School of Thermal Engineering, Shandong Jianzhu University, Jinan, 250101, China
[b] Department of Civil Engineering and Energy Technology, Oslo Metropolitan University, Oslo, N-0130, Norway
[c] School of Environmental Science and Engineering, Tianjin University, Tianjin, 300072, China
[d] Key Lab of Building Environment and Energy of Tianjin, Tianjin University, Tianjin, 300072, China

ARTICLE INFO

Keywords:
Park-level integrated energy system
Long-term planning
Multi-stage divisions
Ladder-type carbon trading mechanism
Linear programming approach

ABSTRACT

The integrated energy system is widely acknowledged as an effective method for advancing the adoption of renewable energy sources and reducing carbon emissions. To address economic issues caused by the inconsistency between traditional single-stage planning capacities of the park-level integrated energy system (PIES), the long-term planning model is proposed, which consists of multi-stage divisions and incorporates the ladder-type carbon trading mechanism. The model utilizes the long-term, multi-stage planning approach to determine the optimal installed capacity of equipment. Meanwhile, the ladder-type carbon trading mechanism is conducted considering the relationship between actual carbon emissions, carbon emission quotas, and carbon trading cost. The study assesses the impact of carbon trading mechanisms and various planning stage divisions on the economic feasibility of the PIES and its ability to reduce carbon emissions. The results indicate that compared to fixed carbon price trading strategies, the implementation of ladder-type carbon trading increases costs by 0.15 %–0.18 %, but reduces carbon emissions by 0.36 %–0.6 %; as the number of planning stages increases, carbon emissions significantly decrease, and lifecycle costs also significantly decrease. Compared to traditional single-stage planning, carbon emissions decrease by 14.6 % and lifecycle costs decrease by 15.17 % at number of planning stage K = 15; when the baseline price is set at 0.5 yuan/kg and the price growth rate is 0.5, the optimal values of carbon emissions and carbon trading cost are achieved. In conclusion, this study serves as references for the strategic implementations of PIES, emphasizing the importance of economic efficiency and low-carbon practices in line with the system's long-term development and sustainability objectives.

1. Introduction

The integrated energy system (IES) aims to integrate and utilize multiple energy resources within a specific region to improve energy utilization efficiency, transform conventional energy consumption patterns, promote the integration of renewable energy sources, achieve multi-system coordination and optimization, and reduce pollution emissions [1,2]. Park-level integrated energy system (PIES) is a specific application of IES, which is rapidly developing in various types of industrial parks across different regions. The construction of clean and low-carbon PIES is becoming a crucial support for facilitating the transition of industries toward low-carbon and sustainable development.

The IES, as a novel integrated energy system capable of meeting diverse energy demands and promoting sustainable energy development, is becoming a prominent research focus in the field of energy engineering. Numerous domestic and international scholars conducted extensive research from various angles and directions. They achieved innovative research outcomes in areas such as model construction, algorithm optimization, capacity configuration optimization and operation. Resulting in numerous targeted recommendations for the optimal economic dispatch of the IES [3,4]. Currently, the modeling research on IES is reaching a relatively mature stage. Based on the different functions performed within the IES, it can be categorized into four modules: energy providers, producers, converters, and consumers [5]. Using the

* Corresponding author. School of Thermal Engineering, Shandong Jianzhu University, Jinan, 250101, China
** Corresponding author. School of Environmental Science and Engineering, Tianjin University, Tianjin, 300072, China.
E-mail addresses: tianzhe@tju.edu.cn (Z. Tian), JXL83@sdjzu.edu.cn (J. Liu).

https://doi.org/10.1016/j.rineng.2024.102107
Received 11 December 2023; Received in revised form 14 March 2024; Accepted 4 April 2024
Available online 8 April 2024

Energy Hub modeling approach, the IES energy network equations are constructed in matrix form, utilizing the Energy Hub structure as a foundation. This enables the transformation of IES's topological structure and energy conversion characteristics into matrix representation [6,7]. Furthermore, a standardized matrix modeling method is proposed, which employs the energy flow between energy equipment as the state variable. This approach facilitates the construction of different source-load equations, considering the unique characteristics of various energy flows, including gas, heat, cold, and electricity. This approach allows for achieving both modeling accuracy and improved computation efficiency [8]. The research on algorithm optimization encompasses every stage of IES planning. Intelligent optimization algorithms can effectively enhance computational efficiency. By enhancing the two-steps k-means algorithm, it is possible to achieve effective clustering, partitioning, and integration of distributed energy resources [9], thereby promoting the wider application of distributed energy resources in IES. Furthermore, the development of multi-objective evolutionary algorithms and modeling methods enables the simulation of annual processes with an hourly time step [10], thus simplifying the computational process and achieving the desired outcomes. IES can achieve the coupling of multiple energy sources, including electricity, gas, and heat. The complex and diverse nature of energy types and conversion equipment further compounds the challenges of capacity allocation. Therefore, the optimization and efficient operation of capacity allocation play a crucial role in maximizing the economic benefits of IES [11]. In order to satisfy the diverse energy requirements of users, it is essential to minimize both system investment and energy cost. Moreover, the planning and design of IES evolved from a singular emphasis on optimizing economic performance [12], to now equally considering both energy efficiency and economic feasibility [13]. Moreover, there is now a growing trend towards a comprehensive approach that incorporates multiple objectives such as economic viability, energy efficiency, and low carbon emissions [14]. This progression contributed to a deepening of the research in the field of IES. Guo et al. [15] examined the configuration and optimization of a distributed energy system which focused on investigating multiple combinations of energy storage and considering both the upper-level equipment configuration and the lower-level energy storage operating parameters. To achieve this, a two-level coordinated optimization approach was employed. Gu et al. [16] developed a two-level decentralized model for low-carbon optimization and scheduling. Carbon emissions effectively reduced through the calculation of this model while also minimizing the economic operational cost of the park ecosystem. These studies utilized a generic two-stage multi-objective planning model and its corresponding solution methods, providing valuable insights for the installed capacity optimization and operation of IES [17]. Overall, the current research on IES spans multiple areas, including model construction, algorithm optimization, installed capacity optimization and operation [18]. These studies achieved a rational allocation of resources and energy, leading to improved computational efficiency and offering important references for further optimization research on IES [19].

The demand for electricity, heating, and cooling load in industrial parks increases as more park users settle in and business profitability grows. This often results in a situation where the equipment capacity of IES is unable to meet the actual load after its implementation. Therefore, it becomes necessary to expand and modify IES according to the specific circumstances [20]. Several scholars have recognized this issue and integrated the concept of medium and long-term planning into the design and implementation of IES [21]. They employed long-term and multi-stage planning techniques to design IES. The accuracy and effectiveness of this model were validated by simulation calculations. Lin et al. [22] proposed a quantitative index for measuring the complementarity of multiple energy sources and applied this index to the long-term planning process of IES. They summarized the relationship between complementarity and economic viability. Additionally, Taheri et al. [23] developed an optimization framework using deep learning algorithms and devised a stepwise algorithm for predicting the operational planning of local energy systems in the medium to long term. Lei et al. [24] proposed a method for determining fluctuation boundaries to analyze and address energy price uncertainty. Through a practical case study, they validated how the sequence of energy hub construction affects the data results of the planning stage. In conclusion, long-term planning theory studied and applied in IES, demonstrating the necessity of such theory [25].

With the establishment of the carbon trading market, some scholars started exploring the IES planning models in the current low-carbon market. Broadly speaking, these explorations can be divided into two aspects. The first aspect focuses on enhancing the system's carbon reduction capacity by implementing Carbon Capture, Utilization and Storage (CCUS) [26,27]. The second aspect studied the carbon generated by IES and carbon trading. Based on the carbon trading mechanism, electricity pricing model, and natural gas pricing model, the carbon trading cost (CTC) is comprehensively calculated considering these mechanisms [28]. For the IES optimization scheduling model considering carbon trading, the carbon emission reduction goals of the system are constrained by the CTC [29].

As demonstrated in Table 1, this study conducted a comparative analysis of previous studies and the present study on IES, with a particular emphasis on energy flow coupling, optimization objectives, and carbon trading. Most of these studies limited their planning horizon to one year [30], neglecting the volatility effects caused by changes in load, weather, and policies. As a result, they fail to adequately demonstrate the long-term effects of energy system planning. Furthermore, during the equipment modeling process, they did not consider the issue of equipment lifespan and the subsequent decline in energy supply quality during later stages of operation. This lack of consideration results in a disconnect between the planning stages and actual operations, limiting the ability to ensure the optimality of the planning solutions [31]. In addition, current research primarily focuses on discussing the optimization of IES planning from an economic perspective, failing to incorporate a thorough examination of the comprehensive impacts of carbon trading, carbon emissions reduction, and other pertinent factors on the long-term planning and operation of IES. Many of these studies treated carbon trading prices as fixed values, meaning they do not change with variations in carbon emissions. There is a limited amount of research analysis on the mechanism of the ladder-type carbon trading (LCT) system, and insufficient attention is given to the urgent issue of reducing carbon emissions in current energy planning. Additionally, it does not take into account the optimized operation of IES under long-term carbon reduction constraints [32].

Based on the above review and the issues identified in previous studies, this study develops a long-term planning model that includes multi-stage partitioning and tiered carbon trading to address the economic and security issues caused by mismatched traditional single-stage planning capabilities. The model considers how different stage divisions can affect the outcomes of the planning process. It takes into account the LCT mechanism and is optimized by minimizing the life cycle cost, serving as the objective function. The study also discusses the influence of factors such as the benchmark price and price growth rates on carbon emissions in the LCT mechanism. Furthermore, a comprehensive PIES optimization solution framework (see Fig. 1) is established based on the relationship between the PIES mathematical model, multi-stage planning model, LCT mechanism model, objective functions, and constraints.

2. Method

2.1. Mathematical model of PIES

Fig. 2 illustrates the structure of the PIES. The external input energy sources include electricity from the grid and natural gas. PIES efficiently meets the demand for heating, cooling, and electricity load of users. The electrical load demand is met by the external grid, photovoltaic (PV), the

Table 1
Comparative analysis of previous studies and the present study on IES.

Reference	Energy flow coupling				Optimization objectives			Carbon trading	
	Electricity	Heat	Cold	Gas	Economy	Low-carbon	Long-term plan	Fixed carbon price	Ladder-type carbon pricing
[11]	✓	✓		✓	✓	✓			✓
[12]	✓	✓	✓		✓				
[13]	✓	✓	✓		✓				
[16]	✓	✓		✓	✓	✓		✓	
[18]	✓			✓	✓				
[22]	✓	✓	✓		✓		✓		
[23]	✓	✓					✓		
[24]	✓	✓		✓	✓	✓			
[28]	✓			✓	✓	✓		✓	
[29]	✓	✓			✓	✓		✓	
This study	✓	✓	✓	✓	✓	✓	✓		✓

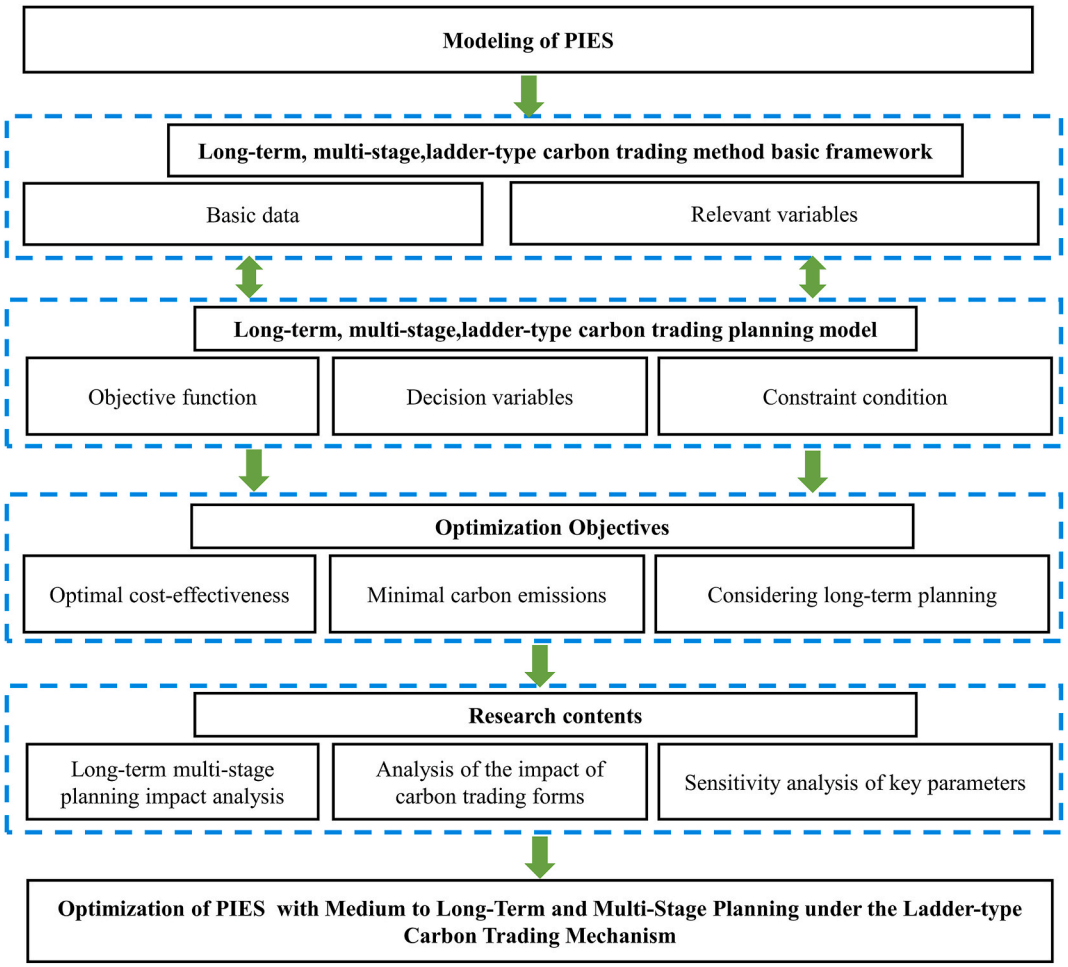

Fig. 1. Optimization solution framework for PIES.

combined heat and power (CHP). The cooling load demand is met through the utilization of the air-source heat pump (HP), electric chiller (EC), absorption chiller (AC). The heating load demand is met by utilizing CHP, gas-fired boiler (GB), and HP. To optimize the economically efficient utilization of regional renewable energy, the energy storage (ES) is configured to manage the inherent uncertainty that arises from the output of renewable energy sources.

2.1.1. Photovoltaic model

The photovoltaic utilizes solar cell materials to convert sunlight into electrical energy, which generates a current. The output power of the system is affected by solar radiation and temperature [33].

$$P_{pv}(t) = Pe_{pv}\eta_{pv}(t)\frac{G(t)}{G_{ref}}[1 + K_T(T(t) - T_{ref}) \quad (1)$$

where Pe_{pv} is the rated power of the PV module, $P_{pv}(t)$ is the electricity output of the PV at time t, η_{pv} is the performance decay coefficient of the PV module, G_{ref} is the solar radiation at standard conditions, $G(t)$ is the actual solar radiation, $T(t)$ is the actual operating temperature, K_T is the temperature coefficient, and T_{ref} is the environmental temperature.

$$T(t) = T_a(t) + \sigma G(t) \quad (2)$$

where $T_a(t)$ is the actual ambient temperature of PV; σ is the radiative

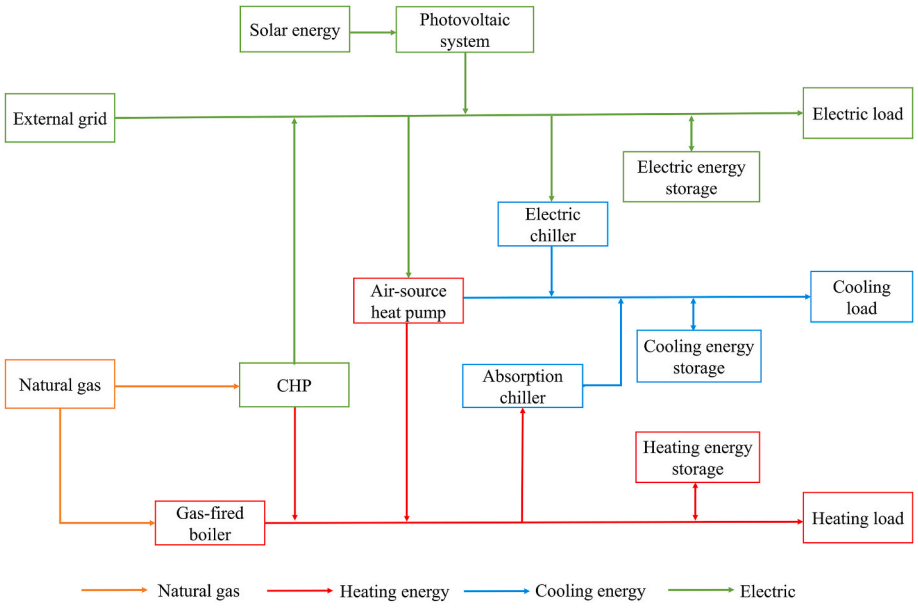

Fig. 2. Structure of the PIES.

temperature coefficient.

2.1.2. Combined heat and power model

CHP consist of Gas Turbine (GT) and waste heat recovery system. The GT utilizes natural gas as fuel to generate both electricity and heat, achieving cascading utilization of energy [32].

$$P_{GT}(t) = \lambda \eta_{GT} V_{GT} L_l \tag{3}$$

where $P_{GT}(t)$ is the electrical power output of the GT; λ is the unit conversion coefficient; η_{GT} is the electrical efficiency of the GT; L_l is the lower heating value of natural gas, and V_{GT} is the natural gas consumption of the GT.

$$H_{GT}(t) = \mu_{re} \eta_{re} P_{GT} \tag{4}$$

where $H_{GT}(t)$ is the heat power output; μ_{re} is the heating-electric ratio of the unit; η_{re} is the heating conversion efficiency of the waste heat recovery system.

2.1.3. Absorption chiller model

AC utilizes heating energy as the driving energy source to achieve the purpose of refrigeration [34].

$$C_{AC}(t) = H_{AC} COP_{AC} \tag{5}$$

where $C_{AC}(t)$ is the cooling power of AC; H_{AC} is the input heating power; COP_{AC} is the coefficient of performance for refrigeration.

2.1.4. Gas-fired boiler model

GB provides heat by burning natural gas and is mainly used as a supplementary heat source to supplement the heating load gap of users [35].

$$H_{GB}(t) = B_{GB}(t) \eta_{GB} \tag{6}$$

where $H_{GB}(t)$ is the heating power of GB; $B_{GB}(t)$ is the energy generated by burning natural gas; η_{GB} is the heating efficiency of GB.

2.1.5. Air-source heat pump model

Air-source heat pump (HP) utilizes high-grade energy to transfer heat from a low-grade heat source, which is the ambient air, to a high-grade heat source. They provide cooling capabilities in the summer and heating capabilities in the winter [36].

$$C^{C}_{HP}(t) = COP_{HP,C} P_{HP}(t) \tag{7}$$

$$H^{H}_{HP}(t) = COP_{HP,H} P_{HP}(t) \tag{8}$$

where $C^{C}_{HP}(t)$ is the cooling power for the HP, $P_{HP}(t)$ is the electrical power consumption, $H^{H}_{HP}(t)$ is the heating power, $COP_{HP,C}$ is the coefficient of performance for cooling, and $COP_{HP,H}$ is the coefficient of performance for heating.

2.1.6. Electric chiller model

EC generates cooling energy by consuming electrical energy [37].

$$C_{EC}(t) = COP_{EC} P_{EC}(t) \tag{9}$$

where $C_{EC}(t)$ is the cooling power of the EC, $P_{EC}(t)$ is the power consumption of the EC, and COP_{EC} is the coefficient of performance of the EC.

2.1.7. Energy storage model

ES systems are integral components of a PIES, as they enhance the system's regulatory capacity and play a crucial role in ensuring safe, stable, and cost-effective system operation [38]. This research primarily focuses on three types of energy storage equipment: heating energy storage (HES), and cooling energy storage (CES) and electrical energy storage (EES).

The mathematical model formula for energy storage equipment s is as follows:

$$E_{ES}(t) = (1 - r) E_{ES}(t-1) + \eta^{ch}_{ES} P^{ch}_{ES}(t) \Delta t - P^{ds}_{ES}(t) \Delta t / \eta^{ds}_{ES} \tag{10}$$

where $E_{ES}(t)$ is the energy stored in the ES. $P^{ch}_{ES}(t)$ and $P^{ds}_{ES}(t)$ are the charging and discharging power, respectively. η^{ch}_{ES} and η^{ds}_{ES} are the charging and discharging efficiencies, respectively. Δt is the time interval, and for this study, it is set to 1 h r is the energy loss coefficient, which is 0.01 for EES, 0.02 for HES, and 0.02 for CES, respectively.

2.2. Modeling of ladder-type carbon trading with long-term, multi-stage planning

2.2.1. Long-term, multi-stage planning model

The multi-stage planning diagram for the PIES is established based on the traditional multi-stage approach as shown in Fig. 3, considering the growth demands of industrial parks loads and carbon emission reduction targets. The planning cycle for the PIES under construction is assumed to be Y years, divided into K stages. Equipment replacement is scheduled based on the lifespan of each equipment, with dashed boxes representing newly installed equipment and solid boxes representing already installed equipment in the diagram. Investments are made at the start of each stage to address load growth, and optimal allocation of equipment installed capacity is conducted for each stage. The planning stage of the previous stage serves as the basis for subsequent stages [39].

In this study, N refers to the number of equipment types. The variable n represents equipment type, where n∈{PV, CHP, AC, GB, HP, EC, ES}, Moreover, a multi-stage sequence, denoted as S, is defined as follows:

$$S = [S_1, S_2, \ldots, S_\alpha, \ldots, S_K] \tag{11}$$

where S_α represents the state of the α, α = 1, 2, …, K.

Corresponding to the stage S_K, the equipment installed capacity allocation matrix is denoted as B_K.

$$B_K = \left[B_n^K\right]_{1\times N} \tag{12}$$

where B_K is the installed capacity allocated for equipment type n in stage S_K.

The cumulative installed capacity allocation matrix for various types of equipment at stage S_K is represented by W_K.

$$W_K = \left[W_n^K\right]_{1\times N} \tag{13}$$

where W_n^K represents the cumulative installed capacity of equipment type n at stage S_K.

2.2.2. Model of ladder-type carbon trading mechanism

In the carbon trading market, the tradeable assets are carbon emission rights or quotas. By setting a maximum limit on carbon emissions and allocating carbon emission quotas (CEQ), legitimate carbon emission rights are established, and their buying and selling are allowed to achieve effective control of carbon emissions [40]. In China's current system, carbon emission allowances are distributed at no cost and allocated using the baseline approach [41]. Within the framework of carbon trading, if a company's actual carbon emissions are lower than the government-allocated quota, the company has the option to trade the surplus carbon quota [42]. In contrast, should the company surpass the allocated quota, it has the option to acquire the excess through the carbon trading market. This study presents a LCT model for carbon trading, which is built upon three crucial elements: actual carbon emissions, CEQ, and CTC.

(1) Model for calculating uncompensated CEQ

The primary contributors to carbon emissions in the IES are the purchase of electricity from the external power grid, the operation of CHP, and GB combustion. This study assumes that all the electricity purchased by the IES from the higher-level power grid is generated exclusively through heating power generation. The baseline method is employed to establish the uncompensated CEQ for the system [43].

$$E_q = E_P + E_{CHP} + E_{GB} \tag{14}$$

$$E_P = \beta_e \sum_{t=1}^{8760} P_{ele}(t)\Delta t \tag{15}$$

$$E_{CHP} = \beta_h \sum_{t=1}^{8760} Q_{GT}(t)\Delta t + \varphi_{e,h} \sum_{t=1}^{8760} P_{GT}(t)\Delta t \tag{16}$$

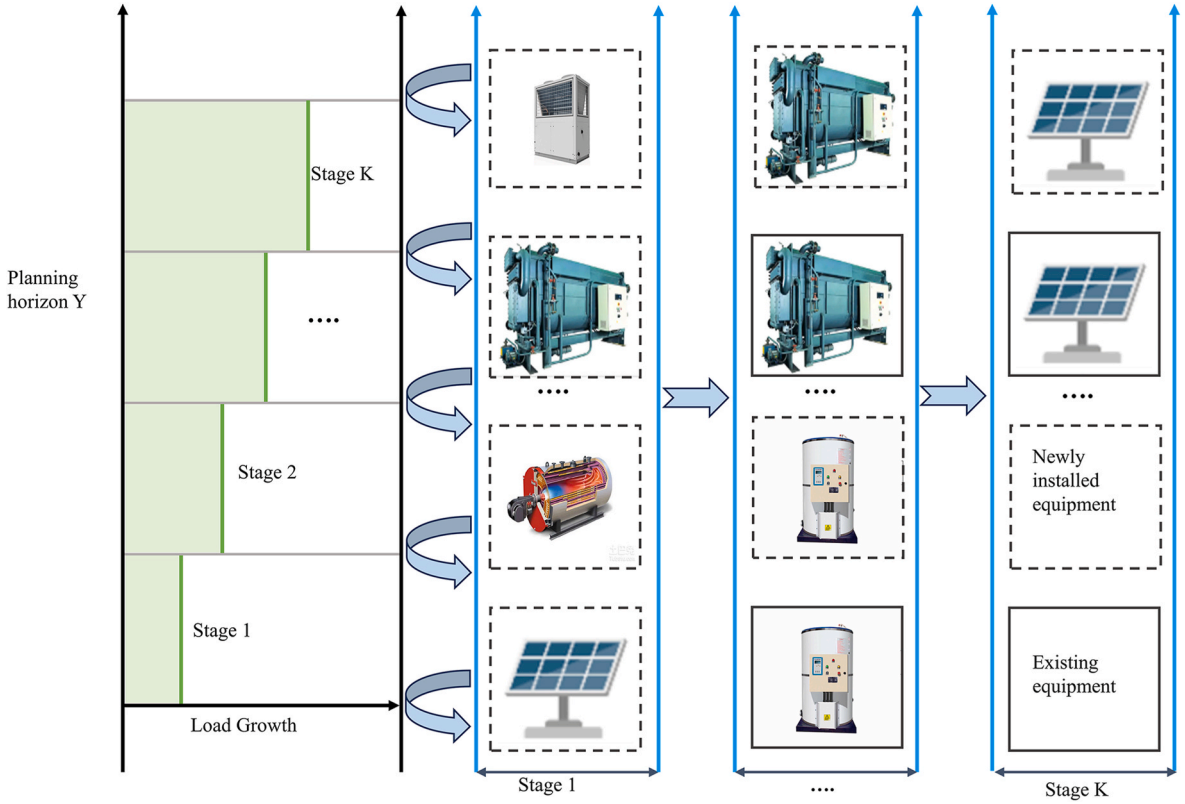

Fig. 3. Diagram of long-term, multi-stage planning method.

$$E_{GB} = \beta_h \sum_{t=1}^{8760} Q_{GB}(t)\Delta t \tag{17}$$

where E_q is the uncompensated CEQ; E_{CHP} is the uncompensated CEQ for CHP; E_P is the uncompensated CEQ for externally purchased electricity; E_{GB} is the uncompensated CEQ for GB. β_e represents the uncompensated CEQ per unit of electricity; P_{ele} (t) is the externally purchased electric power at time t; β_h is the free carbon emission quota per unit of heat; $\varphi_{e,h}$ is the conversion coefficient from the electricity generated by the CHP to the heat generated by it.

(2) Calculation model for actual carbon emissions

To determine the actual carbon emissions resulting from the external grid purchased electricity, CHP operation, and GB combustion, a calculation is performed.

$$E_a = E_{P,a} + E_{CHP,a} + E_{GB,a} \tag{18}$$

where E_a is the actual carbon emissions; $E_{CHP,a}$ is the actual carbon emissions from CHP; $E_{P,a}$ is the actual carbon emissions from purchased electricity; $E_{GB,a}$ is the actual carbon emissions from GB. The calculation methods of $E_{P,a}$, $E_{CHP,a}$, and $E_{GB,a}$ are essentially the same as the formula for calculating carbon emissions quotas, with the difference lying in the values of actual carbon emissions per unit of electricity β_{ea}, and per unit of heat β_{ha}.

(3) Model of the LCT mechanism

The study develops a LCT mechanism, which is based on the correlation between actual carbon emissions and free CEQ. Compared to traditional carbon trading mechanisms, the LCT mechanism can further limit carbon emissions. The difference between actual carbon emissions and free CEQ is divided into multiple trading intervals [44], each interval corresponds to a distinct carbon trading prices, as shown in Fig. 4. When the actual carbon emissions of an industrial park exceed the value of uncompensated CEQ, they must purchase excess quotas from the carbon trading market according to the LCT mechanism. The more CEQ needs to be purchased, the higher the purchase price.

The LCT model is structured as follows:

$$E_{PIES,t} = E_a - E_q \tag{19}$$

$$c_y^{co2} = \begin{cases} \gamma E_{PIES,t} & E_{PIES,t} \le l \\ \gamma(1+\beta)\left(E_{PIES,t} - l\right) + \lambda l & l \le E_{PIES,t} \le 2l \\ \gamma(1+2\beta)\left(E_{PIES,t} - 2l\right) + \gamma(2+\beta)l & 2l \le E_{PIES,t} \le 3l \\ \gamma(1+3\beta)\left(E_{PIES,t} - 3l\right) + \gamma(3+3\beta)l & 3l \le E_{PIES,t} \le 4l \\ \gamma(1+4\beta)\left(E_{PIES,t} - 4l\right) + \gamma(4+6\beta)l & 4l \le E_{PIES,t} \end{cases} \tag{20}$$

where c_y^{co2} is the cost of carbon trading; $E_{PIES,t}$ is the difference between actual carbon emissions and CEQ; γ is the carbon trading benchmark price; l is the length of each emission interval; β is the rate of price growth.

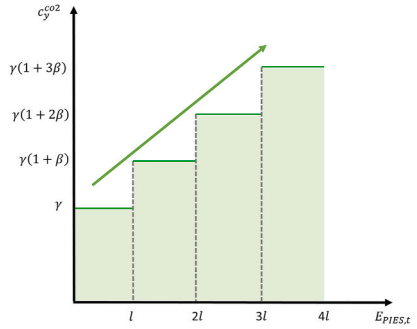

Fig. 4. Diagram of LCT mechanism.

2.3. Optimization model of PIES

2.3.1. Objective functions

The objective function aims to minimize the total regional investment cost c_α^{inv}, equipment residual value c_α^{val}, operating cost c_y^{op}, maintenance cost c_y^{ma}, and carbon trading cost c_y^{co2} throughout the life cycle of the PIES.

$$c_{total} = \sum_{\alpha} \frac{c_\alpha^{inv}}{(1+\varphi)^{y_\alpha - 1}} - \sum_{\alpha} \frac{c_\alpha^{val}}{(1+\varphi)^{Y-1}} + \sum_{y} \frac{c_y^{op}}{(1+\varphi)^{y-1}} + \sum_{y} \frac{c_y^{ma}}{(1+\varphi)^{y-1}} + \sum_{y} \frac{c_y^{co2}}{(1+\varphi)^{y-1}} \tag{21}$$

where y represents the year within the planning period; φ represents the discount rate.

(1) Investment cost model

Investment cost in phase α mainly refers to the equipment investment cost, which is determined by the unit capacity investment cost and the rated installed capacity.

$$c_\alpha^{inv} = \left(\sum_{n=1}^{N} S_\alpha^n M_n \right) \tag{22}$$

where S_α^n is the rated installed capacity of the equipment, and M_n is the unit capacity investment cost.

(2) Equipment residual value model

The study considers the salvage value of equipment that not yet reached its retirement life at the end of the planning period.

$$c_\alpha^{val} = \sum_{n=1}^{N} \left(1 - \frac{(Y+1-y_\alpha)(1-X_n)}{Y_n} \right) S_\alpha^n M_n \tag{23}$$

where X_n represents the net salvage value rate of the nth equipment.

(3) Operating cost model

The research mainly considers the cost of purchasing electricity from the external power grid, selling electricity, and purchasing gas from the higher-level gas network for PIES, which are determined by the actual consumption during system operation.

$$c_y^{op} = \sum_{t=1}^{8760} \left(c_{ele}(t) P_{ele}(t) + c_c(t) P_{ele,c}(t) + c_{gas}(t) V_{gas}(t) \right) \tag{24}$$

where $c_{ele}(t)$ is the purchase price of electricity; $P_{ele}(t)$ is the purchased quantity of electricity; $c_c(t)$ is the selling price of electricity; $P_{ele,c}(t)$ is the quantity of electricity sold; $c_{gas}(t)$ is the price of gas and $V_{gas}(t)$ is the quantity of gas purchased.

(4) Maintenance cost model

The research mainly considers the maintenance cost of PV, energy conversion equipment, and energy storage equipment in PIES, which are determined by the actual output power during the operation of these various types of equipment.

$$c_y^{ma} = \sum_{t=1}^{8760} \sum_{n=1}^{N} \left(c_{ma,n}(t) P_{eq,n}(t) \right) \tag{25}$$

where $c_{ma,n}(t)$ is the unit maintenance cost of the equipment, and $P_{eq,n}(t)$ is the output power of the equipment.

2.3.2. Constraints

Based on the above objective functions, the study considers various constraints, including system energy balance constraint, operational constraints of equipment, and constraints related to ES [45].

(1) System energy balance constraint

The system operation needs to fulfill constraints related to electric power, heating, and cooling balance aspects [46].

Electric power balance:

$$P_{pv}(t) + P_{GT}(t) + P_{ele}(t) + P_{EES}^{ds}(t) = P_{use}(t) + P_{HP}(t) + P_{EES}^{ch}(t) + P_{ele,c}(t) \tag{26}$$

Heating power balance:

$$H_{GB}(t) + H_{HP}^{H}(t) + H_{GT}(t) + H_{HES}^{ds}(t) = H_{use}^{H}(t) + H_{HES}^{ch}(t) + H_{AC}(t) \tag{27}$$

Cooling power balance:

$$C_{AC}(t) + C_{EC}(t) + C_{HP}^{C}(t) + C_{CES}^{ds}(t) = C_{use}^{C}(t) + C_{CES}^{ch}(t) \tag{28}$$

where $H_{use}^{H}(t)$, $C_{use}^{C}(t)$ and $P_{use}(t)$, represent the heating load, the cooling load, and the electrical load at time t, respectively.

(2) Operational constraints of equipment

Long-term, multi-stage planning for equipment operation requires considering the constraints imposed by the cumulative investment capacity at each stage on its operational state [47].

$$0 \le P_i(t) \le P_{i,y}^{max}(t) \le \sum W_{P_i}^{K} \tag{29}$$

$$\sum W_{P_i}^{K} = P_i^1 + P_i^2 + \ldots + P_i^K \tag{30}$$

$$0 \le H_j(t) \le H_{j,y}^{max}(t) \le \sum W_{H_j}^{K} \tag{31}$$

$$\sum W_{H_j}^{K} = H_j^1 + H_j^2 + \ldots + H_j^K \tag{32}$$

$$0 \le C_b(t) \le C_{b,y}^{max}(t) \le \sum W_{C_b}^{K} \tag{33}$$

$$\sum W_{C_b}^{K} = C_b^1 + C_b^2 + \ldots + C_b^K \tag{34}$$

$$y \in K$$

where $P_{i,y}^{max}$, $H_{j,y}^{max}$, and $C_{b,y}^{max}$ represent the upper limits of the rated capacity for power generation equipment, heating equipment, and cooling equipment, respectively. $W_{P_i}^{K}$, $W_{H_j}^{K}$, and $W_{C_b}^{K}$ represent the cumulative capacity of power generation equipment, heating equipment, and cooling equipment in planning stage S_K. The variable y ∈ K denotes that the year y belongs to the stage S_K.

(3) Constraints related to ES

The capacity storage state of ES should meet the upper and lower limit requirements [48].

$$\delta_{ES}^{min} S_{ES} \le E_{ES}(t) \le \delta_{ES}^{max} S_{ES} \tag{35}$$

The energy storage state of ES is equal at the beginning and the end of a day.

$$E_{ES}(0) = E_{ES}(T) \tag{36}$$

The capacity storage state of ES should satisfy the following constraints.

$$\begin{cases} 0 \le P_{ES}^{ds}(t) \le U_{ES}^{ds}(t) P_{ES}^{ds,max} \\ 0 \le P_{ES}^{ch}(t) \le U_{ES}^{ch}(t) P_{ES}^{ch,max} \\ U_{ES}^{ds}(t) + U_{ES}^{ch}(t) \le 1 \end{cases} \tag{37}$$

where $E_{ES}(0)$ and $E_{ES}(T)$ are the capacity stored in the ES at the beginning and end of the time, respectively. $U_{ES}^{ch}(t)$ and $U_{ES}^{ds}(t)$ are binary variables indicating the charging and discharging status. $P_{ES}^{ch,max}(t)$ and $P_{ES}^{ds,max}$ are the maximum charging and discharging power, respectively. S_{ES} is the installed capacity of the ES. δ_{ES}^{min} and δ_{ES}^{max} are the minimum and maximum ranges of the storage state, respectively.

2.4. Model solving methods

The study employed the YALMIP toolbox in the MATLAB environment to call the CPLEX solver for simulating and planning. The simulation and planning consider long-term considerations and involve multi-stage planning, as per the LCT model. The problem is transformed into standard form using linear programming algorithms and solved using the CPLEX solver to obtain the optimal solution [49]. The computational hardware environment employs an Intel(R) Core (TM) i5-12600KF CPU running at 3.70 GHz and is equipped with 32.0 GB of RAM. The specific optimization process is depicted in Fig. 5.

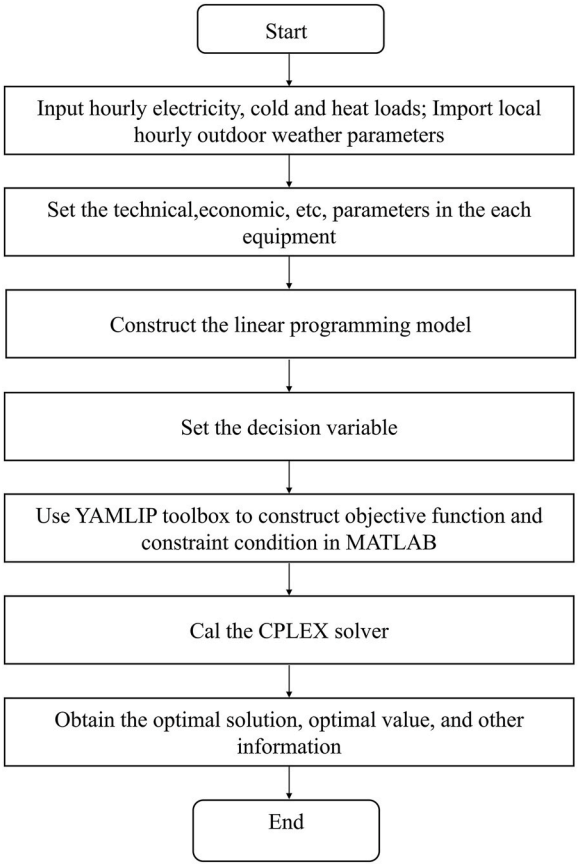

Fig. 5. Diagram of model solving process.

3. Case descriptions

3.1. Parameter settings

(1) Industrial Park loads and energy parameters

The study focuses on a planned industrial park, where three typical days representing summer, winter, and transitional seasons are selected annually [50]. The solar radiation data are obtained from Chinese Standard Weather Data (CSWD) [51], and the solar radiation data for these three typical days can be seen in Fig. 6. Since solar radiation is minimally affected by climate change, it is assumed to remain constant throughout the entire planning period. The planning period covers a span of 15 years, with equipment investment divided into a maximum of 15 stages. The initial yearly load demand for the selected typical days is illustrated in Fig. 7. Moreover, taking into account the anticipated increase in load due to the addition of new users and the improvement of enterprise efficiency, the projected demands for electricity, heating, and cooling within the park are expected to experience an average annual growth rate of 2.0 % over the planning period.

The planned area is connected to the external power grid and external gas network, with the electricity price being determined on the basis of the annual electricity price provided by the grid operator. A time-of-use electricity pricing model, as illustrated in Fig. 8, is utilized. The purchase price for natural gas is set at 3.3 CNY/Nm^3.

(2) Equipment parameters

Table 2 provides the investment cost, operating and maintenance cost, and service life parameters of PV and energy conversion equipment within the industrial park [52]. The technical and economic parameters of ES are shown in Table 3 [53]. The technical and economic parameters of energy equipment can be found in Table 4 [54,55].

3.2. Case settings

In this study, a long-term, multi-stage planning model is developed using the LCT mechanism. Three primary scenarios are developed for simulation calculations to investigate and analyze the effects of carbon trading form, number of planning stages, and variations in LCT parameters on regional comprehensive energy system planning. These scenarios are shown in Table 5.

The first category of scenarios examines the impact of different forms of carbon trading on the planning process. Specifically, we compare the influences of two distinct types of carbon trading: fixed carbon prices and LCT. These scenarios are denoted as case 1 to case 4.

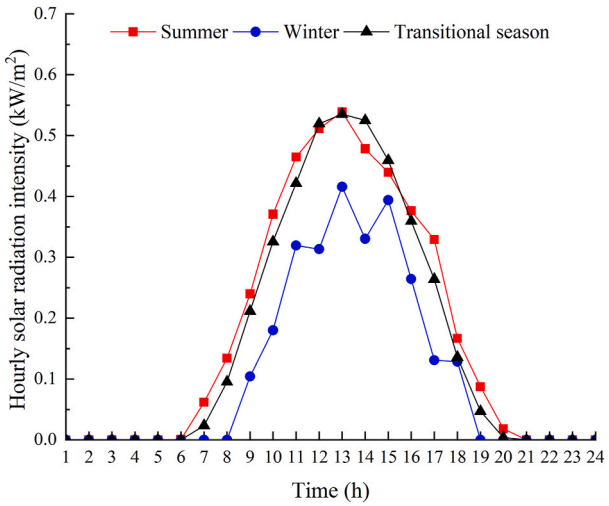

Fig. 6. Hourly solar radiation intensity.

The second category of scenarios investigates the impact of the number of planning stages. These scenarios, designated as case 5 through case 8, all utilize the LCT mechanism. The primary distinction among them is the varying number of planning stages. Specifically, in case 5, there is one planning stage (K = 1). In case 6, there are three planning stages (K = 3). In case 7, there are five planning stages (K = 5). Lastly, in case 8, there are fifteen planning stages (K = 15).

The third category of scenarios investigates the impact of varying parameters in the LCT mechanism. Specifically, we examine the effects of variations in the benchmark price γand the price growth rate βon the operation of the system. In case 9, we focus on evaluating the influence of variations in the benchmark price. To accomplish this, we set the baseline price to a range of 0.1–0.5 CNY/kg, with a step size of 0.05 CNY/kg, and used the simulation calculation framework established in case 4. On the other hand, case 10 analyzes the effects of adjustments in the price growth rate. The range of variation for the price growth rate was set from 0.1 to 0.5 %, with a step size of 0.05 %. The simulation calculations are conducted by modifying the price growth rate within the framework outlined in case 4.

4. Results

4.1. Analysis of the impact of carbon trading form

Considering the eight typical cases of scenario one and scenario two, namely case 1 to case 8, the PIES is optimized and configured. The planning cost, equipment installed capacity, and carbon emissions of the 8 cases are obtained over a span of 15 years.

Table 6 presents the cost comparison of four cases, namely case 1 to case 4. According to Tables 6 and it is evident that the cases implementing the LCT mechanism experience an increase in life cycle cost. Further analysis reveals that case 2 demonstrates a 0.18 % increase in comparison to case 1, while case 4 displays a 0.15 % increase relative to case 3. Nevertheless, it is important to highlight that the cost of carbon trading experiences a significant decrease. Case 2 demonstrates an 11.14 % decrease compared to case 1, and case 4 exhibits an 8.57 % decrease compared to case 3.

Fig. 9 illustrates the optimal allocation of equipment installed capacity for the four cases (case 1 to case 4). It is evident from the figure that cases EC and GB, which implement the LCT mechanism, have lower installed capacity, whereas cases GT and HES increase installed capacity. More specifically, in case 2, the installed capacity of GB decreases by 584.68 kW compared to case 1, while in case 4, it decreases by 245.01 kW compared to case 3. In contrast, in case 2, the installed capacity of GT increases by 225.62 kW compared to case 1, and in case 4, it increases by 60.44 kW compared to case 3. GT, being the core equipment for energy cascade utilization, has the capability to provide both electricity and heat, thus reducing the high carbon emissions associated with purchasing external electricity and mitigating the use of high carbon emission equipment like GB. Therefore, the LCT mechanism is more effective in responding to carbon emission constraints, as it effectively reduces the usage of high carbon emission equipment and minimizes carbon dioxide emissions during system operation.

Fig. 10 shows the cumulative carbon emissions for the four cases, case 1 to case 4. Upon observing Fig. 9, it becomes apparent that carbon emissions experience a notable decrease across all the cases. Specifically, case 2 has a carbon emission decrease of 0.36 % compared to case 1, while case 4 displays a carbon emission decrease of 0.6 % compared to case 3. This is due to the implementation of the LCT mechanism in both case 4 and case 2. The ladder-type carbon pricing results in higher carbon trading prices within the high-carbon-emission range as opposed to the fixed carbon price trading. Consequently, the proportion of CTC increases, leading to a natural reduction in the construction and utilization of high-carbon-emission equipment.

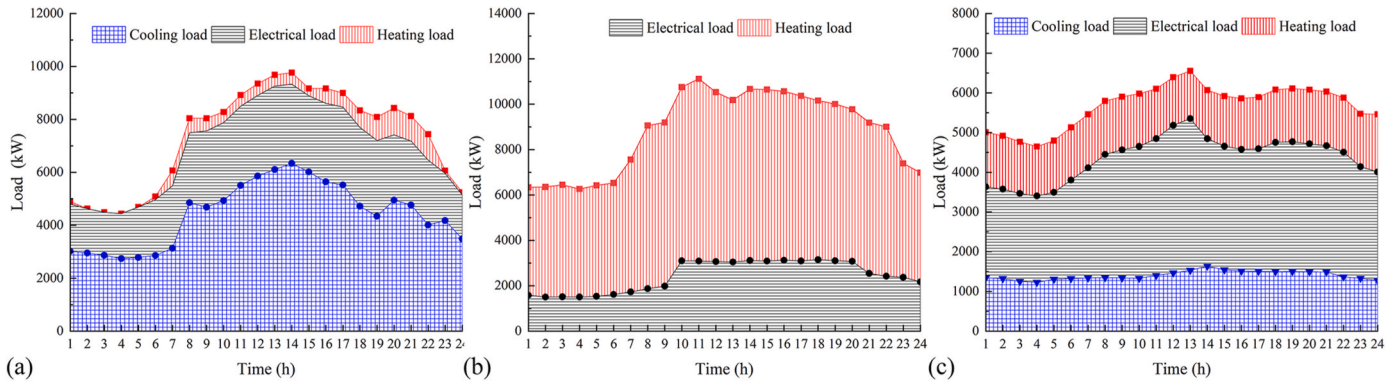

Fig. 7. Typical daily load. (a) Typical day in summer, (b) typical day in winter, (c) typical day in transitional season.

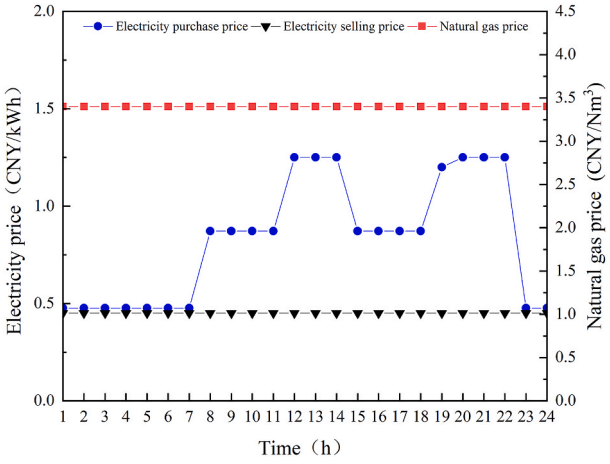

Fig. 8. The energy prices.

Table 2
Technical and economic parameters of energy equipment.

Type	Efficiency	Initial cost (CNY/kW)	Maintenance cost (CNY/kWh)	Equipment life (a)
PV	–	10000	0.03	20
CHP	power generation:0.43 heating conversion:0.8	9000	0.08	20
AC	1.3	1300	0.01	20
EC	3	900	0.02	20
GB	0.95	800	0.01	20
HP	cooling:4 heating:3	3200	0.02	20

Table 3
Technical and economic parameters of ES.

Type	State range	Charging and discharging efficiency	Initial cost (CNY/kW)	Maintenance cost (CNY/kWh)	Equipment life (a)
EES	0.1–0.9	0.95/0.95	1100	0.05	10
HES	0.1–0.9	0.95/0.95	500	0.03	20
CES	0.1–0.9	0.95/0.95	500	0.03	20

4.2. Analysis of the impact of number of planning stages

Considering the four typical configurations (case 5~case 8) in scenario 2, the PIES was optimized to obtain the equipment installed capacity results for each stage of the four cases in scenario 2, as well as the corresponding life cycle cost. From the table outlining the different case configurations in Tables 5 and it is evident that all four cases (case 5~case 8) utilized the LCT mechanism, with the only difference being the quantity during the planning stage.

Table 4
Additional calculated parameters related to each equipment.

Parameters	Value	Parameters	Value
G_{ref}	1000 W/m^2	L_l	34920 kJ/Nm^3
K_T	−0.35 %/°C	μ_{re}	1.125
T_{ref}	25 °C	φ	0.07
σ	0.0256	X_n	7 %
λ	$\frac{1}{3600}$ kWh/kJ	β_e	0.728 t/MWh
$\varphi_{e,h}$	6 MJ/kWh	β_h	0.367 t/MWh
β_{ea}	1.08 t/MWh	β_{ha}	0.327 t/MWh

Table 7 presents a comparison of the planning cost for cases 5 to 8. It is evident from the table that the investment cost of the four cases accounted for approximately 37 %–45 % of the life cycle cost. On the other hand, the operating cost constituted around 58 % of the life cycle cost. In comparison, the equipment's residual value, maintenance cost, and CTC made up a relatively smaller proportion. As the number of planning stages increased, the operating and maintenance cost of the equipment consistently decreased. Specifically, in case 8, there is a 15.35 % decrease in maintenance cost compared to case 5, amounting to 3,997,507.36 CNY. Furthermore, the residual value of the equipment consistently increases, resulting in a declining trend in total system cost. The more planning stages there were, the lower the overall system cost become. In case 8, there is a 15.17 % decrease in life cycle cost compared to case 5, which equates to a reduction of 52,934,142.8 CNY. This can be attributed to the fact that case 5 has the fewest number of planning stages, with a value of K = 1. Conversely, the other cases follow a multi-stage planning model, with case 8 having the highest number of planning stages at K = 15. Fewer planning stages in a case leads to increase investment and maintenance cost. This is because the equipment is constructed in the initial year based on the projected load demand for the final year. Additionally, the extended usage period and lack of equipment updates result in a lower equipment recovery value and residual value. In contrast, the multi-stage planning models allow for a more reasonable investment in equipment based on the load demand for each stage, resulting in higher recoverable value and an increase in residual value over time.

Fig. 11 depicts the installed capacity at different planning stages for case 6 and case 7. By the end of the planning period, it is evident that case 7 has higher total installed capacity for PV, CHP, EC, HP, and EES compared to case 6. The total installed capacity for AC is similar in both cases. However, case 7 has lower installed capacity for GB and HES compared to case 6. Remarkably, the largest disparity in installed

Table 5
Settings of different scenarios.

Cases		Different forms of carbon trading		Planning stage K				Parameters of ladder-type carbon trading	
		Fixed carbon prices	Ladder-type carbon trading	1	3	5	15	Benchmark price	Price growth rate
Scenarios one	case 1	✓		✓					
	case 2		✓	✓					
	case 3	✓			✓				
	case 4		✓		✓				
Scenarios two	case 5		✓	✓					
	case 6		✓		✓				
	case 7		✓			✓			
	case 8		✓				✓		
Scenarios three	case 9		✓		✓			✓	
	case 10		✓		✓				✓

Table 6
Comparison of the planning cost for cases 1 to 4.

Case	Life cycle cost/$\times 10^6$ CNY	Investment cost/$\times 10^6$ CNY	Equipment residual value/ $\times 10^6$ CNY	Operating cost/$\times 10^6$ CNY	Maintenance cost/$\times 10^6$ CNY	Carbon trading cost/ $\times 10^6$ CNY
case 1	348.36	132.12	14.15	201.53	25.62	3.23
case 2	349.00	130.85	14.36	203.60	26.04	2.87
case 3	307.76	117.13	14.07	179.57	22.59	2.54
case 4	308.21	117.00	14.27	180.31	22.84	2.33

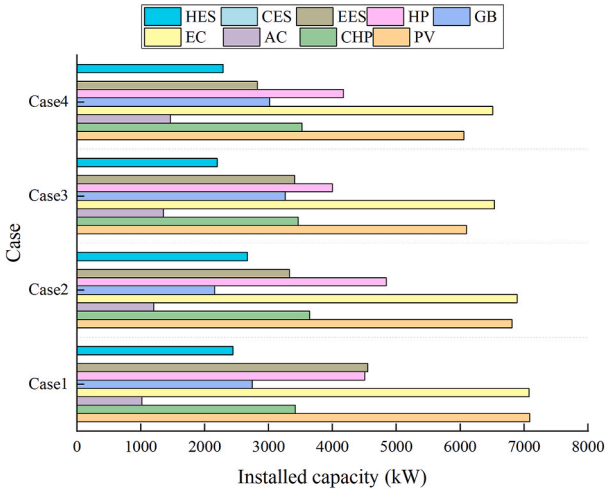

Fig. 9. Optimal equipment installed capacity allocation of cases 1 to 4.

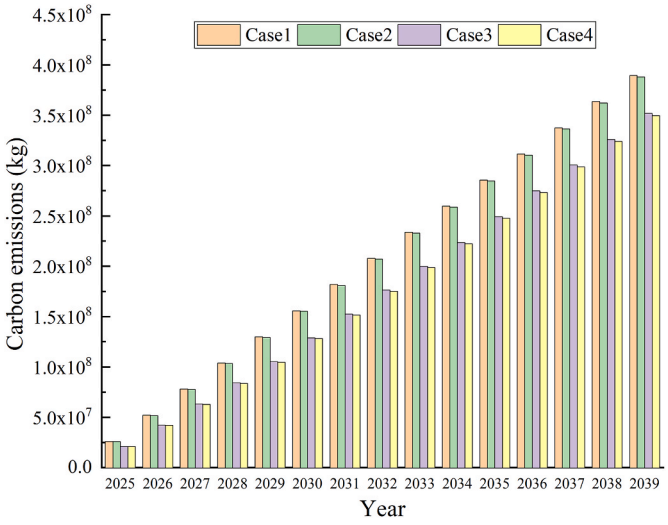

Fig. 10. Accumulated carbon emissions of cases 1 to 4.

capacity is observed in PV, with case 7 exhibiting an increase of 743.79 kW compared to case 6. Despite case 7 having higher total installed capacity for most equipment in comparison to case 6, its life cycle cost is lower by 0.74 %. This reduction can be attributed to the effectiveness of a multi-stage planning method in responding to the changing load demands over the years. This approach minimizes the risk of investing prematurely in redundant equipment by strategically planning and gradually increasing equipment installation. As a result, both the cost of equipment investment and maintenance are effectively reduced. Furthermore, at the conclusion of the planning period, it is evident that case 7 has a higher remaining useful life for its equipment compared to case 6, leading to a commendable 24 % increase in equipment residual value. Therefore, the multi-stage planning method proves highly effective in optimizing the overall economic viability of the PIES.

We conducted an analysis on the impact of multi-stage divisions, specifically under the LCT mechanism, on low-carbon performance. Fig. 12 illustrates the carbon emissions for different cases during the planning period from case 5 to case 8. It is evident that with an increasing number of stages, there is a continuous decrease in carbon emissions. When comparing case 5, which represents the traditional single-stage division, with case 8, divided into 15 stages, it is evident that the carbon emissions in case 8 decrease by 49425384.14 kg, or 14.6 %. Furthermore, the overall economic analysis of the system mentioned earlier reveals a consistent decrease in the life cycle cost as the number of stages increases. Therefore, a comprehensive analysis of the eight typical cases leads to the conclusion that the long-term, multi-stage LCT model proposed in this study positively impacts the reduction of carbon emissions, promotion of new energy consumption, and lowering of the overall life cycle cost of the system.

Table 7
Comparison of the planning cost for cases 5 to 8.

Case	Life cycle cost/10^6 CNY	Investment cost/10^6 CNY	Equipment residual value/10^6 CNY	Operating cost/10^6 CNY	Maintenance cost/10^6 CNY	Carbon trading cost/10^6 CNY
case 5	349.00	130.85	14.36	203.60	26.04	2.87
case 6	308.21	117.00	14.27	180.31	22.84	2.33
case 7	305.93	121.05	17.72	177.36	22.79	2.45
case 8	296.07	133.13	35.54	174.62	22.04	2.31

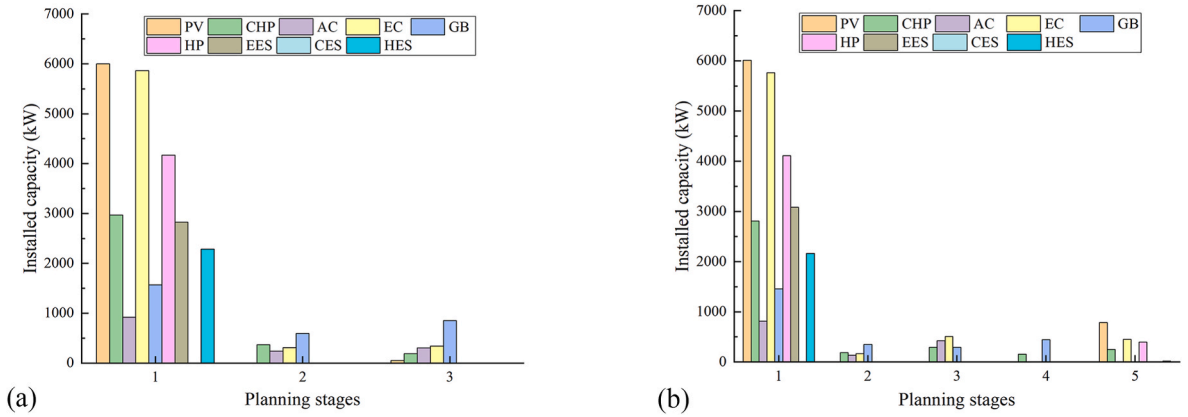

Fig. 11. Comparison of installed capacity in different planning stages between case 6 and case 7. (a) Installed capacity at different planning stages in case 6, (b) Installed capacity at different planning stages in case 7.

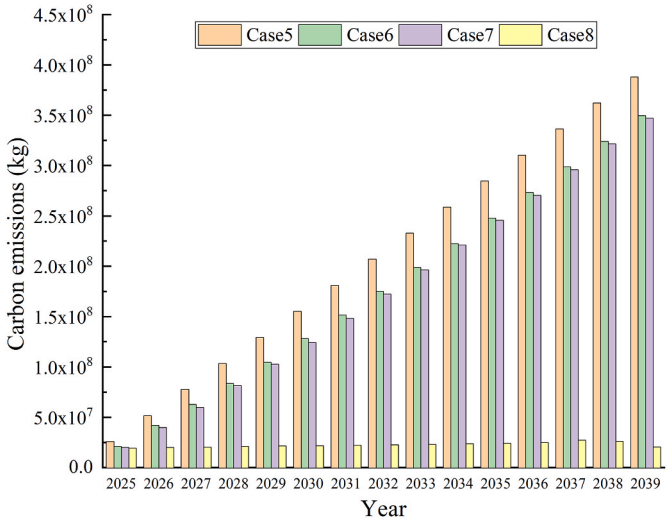

Fig. 12. Accumulated carbon emissions of cases 5 to 8.

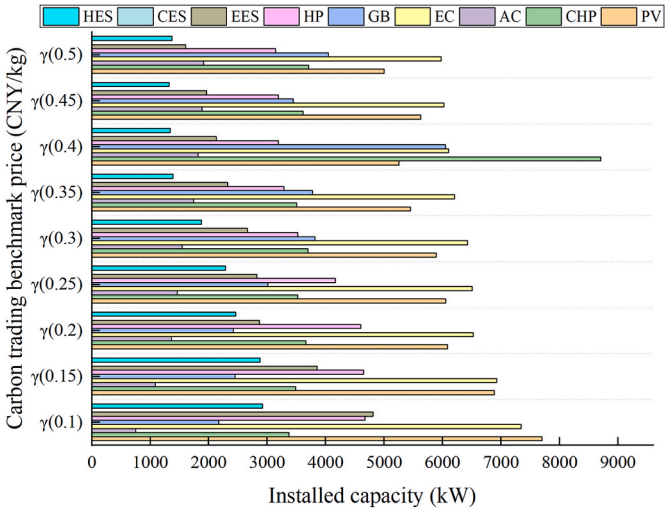

Fig. 13. Equipment installed capacity under different benchmark price of carbon trading for case 4.

4.3. Sensitivity assessment of the parameters in the carbon trading system

4.3.1. Impact of benchmark price on carbon trading

By modifying the benchmark price in accordance with case 4, the varying effects of this modification on carbon emissions and CTC can be analyzed.

Fig. 13 illustrates the impact of different benchmark prices on the configuration of equipment's installed capacity. The analysis reveals a clear trend: as the benchmark price rises, the total installed capacity of GT, AC, and GB experiences a continuous rise, while the total installed capacity of PV, EC, HP, EES, and HES consistently declines. Remarkably, AC experiences the most significant increase in total installed capacity, with a maximum rise of 61 %. Conversely, EES exhibits the largest decline, with a maximum decrease of 67 %. These findings indicate that an increase in the benchmark price has a greater influence on the system's operations, particularly regarding carbon emissions. Consequently, the system reduces investments in electrical equipment to mitigate high carbon emissions associated with electricity consumption. Conversely, the construction of GT, which can provide both electrical and heating energy simultaneously, and the development of high-efficiency GB are emphasized. This strategic shift aims to effectively mitigate the system's carbon emissions by meeting the heating load demand of users and providing a heat source for AC usage.

Fig. 14 illustrates the variations in carbon emissions and CTC at different benchmark prices. As the benchmark price increases, the overall trend of carbon emissions initially increases, then stabilizes, and finally decreases. Similarly, the overall trend of CTC initially decreases, then increases, and finally decreases again. At a benchmark price of 0.2 CNY/kg, the carbon emissions reach their maximum value. At a

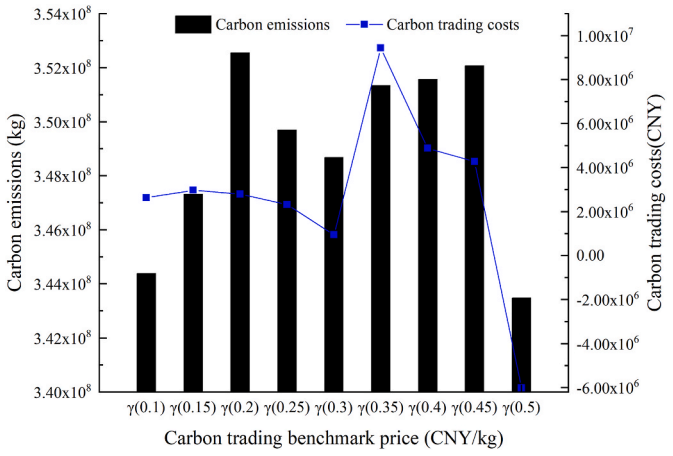

Fig. 14. Changes in carbon emissions and CTC under different benchmark price for case 4.

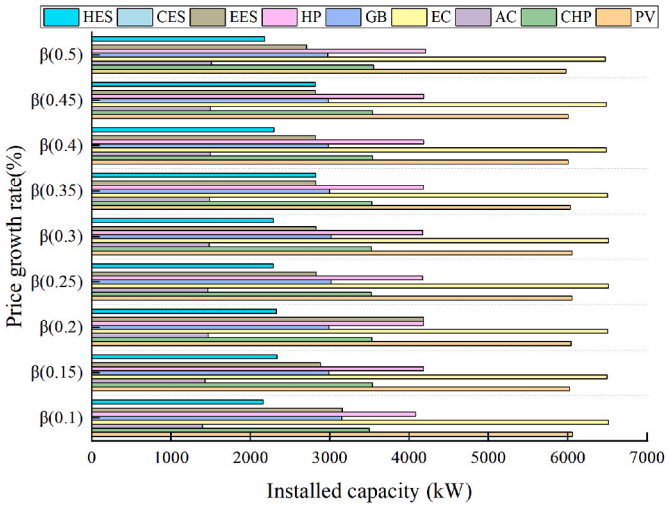

Fig. 15. Equipment installation capacity allocation under various rates of price growth of carbon trading for case 4.

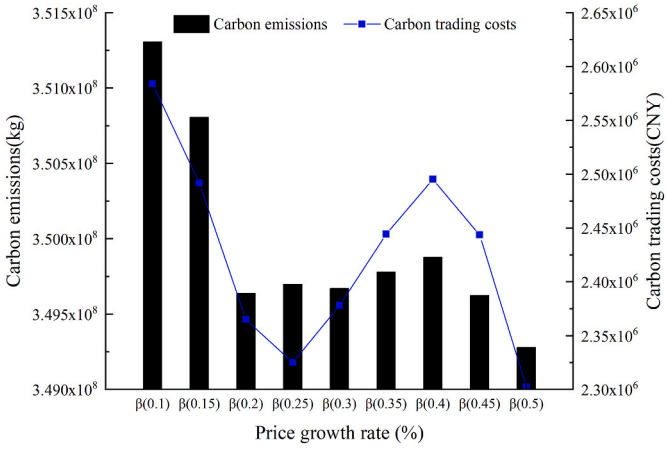

Fig. 16. Changes in carbon emissions and CTC under various rates of price growth for case 4.

benchmark price of 0.35 CNY/kg, the CTC reach their maximum value. At a benchmark price of 0.5 CNY/kg, both the carbon emissions and CTC reach their minimum values. This primarily involves a trade-off in the system optimization process between the cost of purchasing external electricity and the life cycle cost of electricity generation from the PIES. When the benchmark price is low, the system places less emphasis on carbon emissions and prioritizes economic considerations, resulting in a lower cost of purchasing electricity. Consequently, the system relies more on external electricity procurement. However, this trend results in additional CTC, leading to a gradual increase in carbon emissions and subsequent carbon trading expenses. As the benchmark price for carbon trading increases, there is a corresponding rise in the proportion of CTC. Consequently, the overall cost of electricity generation within the system becomes lower than the cost of purchasing electricity. Consequently, the system starts reducing its dependence on external electricity procurement. The economic benefits derived from purchasing external energy are insufficient to offset the high CTC. In response, PIES adjusts its energy consumption pattern by increasing the proportion of clean energy usage and reducing reliance on external energy. This effectively reduces carbon emissions and lowers CTC.

4.3.2. Impact of price growth rate on carbon trading

This study explores the effects of different rates of price growth on carbon emissions and the cost associated with carbon trading, using case 4 as a basis for analysis.

Fig. 15 presents the configuration of installed capacity for different equipment under varying rates of price growth. The findings reveal that as the rate of price growth increases, the total installed capacity of GT and HP also increases. In contrast, the total installed capacity of GB and EES shows a downward trend. Additionally, the total installed capacity of PV and EC remains relatively stable.

Fig. 16 illustrates the fluctuation in carbon emissions and CTC across different rates of price growth. It is evident that as the rate of price growth increases, there is an initial decrease in carbon emissions, followed by an increase, and then another decrease. Likewise, the trend in CTC follows a similar pattern of initially decreasing, followed by an increase, and then another decrease. When the growth rate is 0.1, both carbon emissions and CTC reach their maximum values. Conversely, at a growth rate of 0.5, both carbon emissions and CTC reach their minimum values. Notably, at price growth rates of 0.25 and 0.4, both carbon emissions and CTC exhibit inflection points. When the price growth rate is low, the total system generation cost surpasses the cost of procuring electricity from external sources. To achieve the most economically efficient outcome, the system chooses to purchase electricity externally, which results in higher carbon emissions and CTC. However, as the price growth rate increases, the cost of carbon trading also rises. This results in a higher proportion of CTC in the overall cost structure. Consequently, the system becomes more sensitive to carbon emissions, eventually leading to a scenario where the total cost of electricity generation by the system becomes lower than the cost of purchasing electricity from external sources. To maximize economic efficiency, the system starts reducing its reliance on external electricity purchases, leading to a decrease in carbon emissions and a reduction in CTC. As the growth rate continues to increase, there is a decrease in external electricity purchases. To meet user demand for power, the use of GT equipment leads to an increase in carbon emissions. Moreover, as the growth rate exceeds 0.4, the system faces stronger constraints on carbon emissions. Therefore, the proportion of CTC continues to increase steadily. Consequently, the system implements restrictions on the use of high-carbon emitting equipment, resulting in decreases in both carbon emissions and CTC.

5. Discussion

This study examines the adoption of the LCT mechanism and a fixed carbon price trading mechanism. The findings reveal that under the LCT mechanism, there is an increase in CTC as carbon emissions also increase. This leads to a higher proportion of CTC. This subsequently prompts a reduction in the utilization of high-carbon emitting equipment. The installed capacity of EC and GB devices decreases, while that

of GT and PV devices increases. Consequently, carbon emissions show a declining trend. Therefore, the implementation of the LCT mechanism positively contributes to carbon reduction efforts and effectively enhances the low-carbon nature of the PIES.

The findings indicate a consistent decline in carbon emissions, life cycle cost, operating cost, and maintenance cost with an increase in the number of planning stages. Furthermore, the residual value of the equipment shows a continual increase. The total installed capacity of PV, which emits zero carbon, and GT, which allows for cascaded energy utilization, also increases. Furthermore, there is a continuous increase in the installed capacity of EES, facilitating peak shaving and valley filling. As a result, adopting a multi-stage planning model has the potential to enhance the overall economic viability of PIES and contribute to a sustained reduction in carbon emissions. Therefore, the model proposed in this study can effectively reduce carbon CO_2 emissions and improve economic sustainability.

The study implements CES as the cooling energy storage device, but it is not utilized during system operation. Our analysis reveals the reasons for this. Firstly, we use AC, HP, and EC equipment to meet the cooling load requirements, with the HP device running continuously throughout the day. Secondly, utilizing peak and off-peak electricity rates for cooling energy storage and discharge incurs higher economic costs and lower energy utilization efficiency compared to direct energy storage. Therefore, to reduce operational costs, improve energy utilization efficiency, and minimize carbon emissions, the system chooses to forego the use of CES and instead implements EES for cold energy management.

The planning method and research model obtained in this study can provide inspiration and guidance for PIES planners, but there are still some shortcomings. The study fails to adequately consider the fluctuating effects of economic factors. Firstly, it overlooks the impact of energy price fluctuations, including electricity and gas prices. In reality, the determination of energy prices requires consideration of various factors [56]. Given the changing international environment and advancements in clean energy generation and natural gas extraction technologies, electricity and gas prices are not constant. These fluctuations in energy prices can also have an impact on the carbon trading market. Secondly, the study neglects the influence of inflation rates on the cost of equipment replacement in industrial parks. Therefore, it is imperative to allocate due consideration to the dynamic impact of economic factors when strategizing for PIES. This is essential to guarantee a thorough and precise analysis.

The study fails to assess the impact of uncertainties and the level of uncertainty on the long-term planning of PIES [57]. For example, climate change and weather fluctuations can cause variations in PV output, thus affecting the output of PV energy generation units. Additionally, the intermittent and unpredictable nature of renewable energy sources can also affect the installed capacity of the energy system, leading to a range of operational outcomes [58]. Furthermore, the study only considers a 2.0 % annual average growth rate for electrical, heating, and cooling loads during the planned period. However, the actual load variations within the industrial parks are far more complex, as the study fails to consider the significant increase in loads resulting from the influx of large industrial users.

Hydrogen plays a crucial role in modern energy systems. Hydrogen-powered vehicles, especially in the public transportation sector, are being widely adopted [59,60]. Looking towards the future, there is considerable potential for further research and application of hydrogen energy in industrial parks. Additionally, the use of electric vehicles led to an increase in the electrical load of the PIES [61]. It is worth noting that some industrial parks are achieving full coverage of charging stations. Consequently, it is crucial to consider the resulting load variations from the widespread use of hydrogen energy and electric vehicles in future research. This would help in exploring new optimization strategies for the configuration of PIES.

Under dual carbon targets, CCUS technology is attracting attention from scholars for research [62]. CCUS technology allows for the capture and purification of carbon dioxide emitted during the production process, followed by its integration into new production processes for recycling or storage. Currently, CCUS technology is primarily applied in industries with significant emission reduction challenges, such as steel plants, cement plants, and chemical industries, with the goal of achieving zero carbon emissions. It is primarily utilized in industrial demonstration projects [63]. Therefore, integrating CCUS technology in research on optimizing PIES can effectively reduce CO_2 emissions and enhance the system's low-carbon characteristics [64]. For instance, the implementation of carbon capture technology in a combined heat and power plant not only enhances its flexibility, but also improves its low-carbon nature and economic efficiency [65]. In the scenario of wind power grid integration, wind power generation can be used to provide electricity for carbon capture devices, enabling improved integration of renewable energy into the system, reducing wind curtailment rates, and achieving low-carbon operation [66]. In addition, CCUS technology can be utilized to react captured carbon dioxide with natural gas, resulting in the production of hydrogen. This method offers a low carbon emissions profile during production and can effectively meet the energy demands of industries and buildings without generating additional carbon emissions during usage. Therefore, it is crucial to actively develop this methodology to fulfill the energy needs of various sectors. Furthermore, exploring how to incorporate the dual carbon targets into design by setting planning deadlines holds practical significance. As a result, further research is required to delve deeper into these issues.

6. Conclusion

This study presents a comprehensive long-term planning model for an industrial park. The model considers multi-stage variations and incorporates the LCT mechanism. The study thoroughly examines the influence of long-term planning theory on the operation of PIES. In contrast to previous studies that usually have a one-year planning horizon, this research extends the planning period to 15 years. Moreover, this study comprehensively examines the effects of load variations on system stability and the influence of equipment lifespan on operational efficiency. This allows for an in-depth analysis of the long-term operation of PIES. In contrast to previous studies that primarily focus on optimizing PIES from an economic perspective, this study introduces a LCT mechanism. By considering the cost associated with carbon trading, this mechanism imposes constraints on carbon emissions, ultimately facilitating optimized operations of PIES that align with long-term carbon reduction objectives. The study further investigates three distinct scenarios, exploring and analyzing the impacts of carbon trading mechanisms, the number of planning stages, and variations in LCT parameters on the planning of regional comprehensive energy systems. The key findings are summarized as follows.

(1) Compared to trading strategies with fixed carbon prices, the implementation of LCT increases costs by 0.15–0.18 %, but reduces carbon emissions by 0.36–0.6 %. The use of LCT mechanisms effectively limits carbon emissions from PIES, despite the increase in costs. Moreover, the implementation of the LCT mechanism results in an increase in installed capacity of clean energy devices. This signifies a positive impact on the integration of new energy sources and the promotion of renewable energy in the energy mix.

(2) The division of planning stages can effectively avoid equipment redundancy and reduce the operation and maintenance costs of equipment. As the number of planning stages increases, carbon emissions significantly decrease, and lifecycle costs also decrease significantly. Compared to traditional single-stage planning, when the number of planning stages $K = 15$, carbon emissions decreased by 14.6 %, and lifecycle costs decreased by 15.17 %. Therefore, in the long-term planning of PIES, dividing the

planning stages reasonably can effectively reduce carbon emissions while lowering the overall costs involved.

(3) Both the carbon emissions and CTC of the system are highly responsive to variations in the benchmark price and price growth rate. An increase in the benchmark price and price growth rate leads to greater volatility in the trends of system carbon emissions and CTC. The optimal values for carbon emissions and CTC are achieved when the benchmark price is set at 0.5 CNY/kg and the price growth rate is 0.5. It is, therefore, crucial to appropriately determine the benchmark price and price growth rate to achieve low-carbon operation and economic benefits for PIES.

In conclusion, this study can provide valuable reference for the long-term planning of low-carbon PIES. However, the considerations regarding energy price fluctuations, load growth rates, and other factors are not comprehensive enough, and further in-depth research is needed in the future. In addition, the development of technologies such as hydrogen energy, electric vehicles, CCUS, etc., poses new challenges for PIES, which will be an important direction for future research.

CRediT authorship contribution statement

Kaiyue Li: Writing – review & editing, Writing – original draft, Methodology, Investigation, Formal analysis, Data curation, Conceptualization. **Jingyu Ran:** Writing – review & editing, Software, Resources, Investigation, Formal analysis, Data curation. **Moon Keun Kim:** Writing – review & editing, Validation, Supervision. **Zhe Tian:** Writing – review & editing, Validation, Supervision, Project administration, Investigation. **Jiying Liu:** Writing – review & editing, Validation, Supervision, Project administration, Investigation, Funding acquisition.

Declaration of competing interest

The authors declare that they have no known competing financial interests or personal relationships that could have appeared to influence the work reported in this paper.

Nomenclature

Abbreviation	
AC	absorption chiller
CE	carbon emissions
CEQ	carbon emission quotas
CES	cooling energy storage
CHP	combined heat and power
CTC	carbon trading cost
HES	heating energy storage
EC	electric chiller
ES	energy storage
EES/ /	electrical energy storage
GB	gas-fired boiler
GT	gas turbine
HP	air-source heat pump
LCT	ladder-type carbon trading
PV	photovoltaic
Symbols	
B_K	the capacity allocated in stage S_K
$B_{GB}(t)$	energy generated by burning natural gas, kW
C	cooling power, kW
COP	unit coefficient of performance
E	actual carbon emissions or uncompensated carbon emission quota, kg
$G(t)$	actual solar radiation, W/m^2
G_{ref}	solar radiation at standard conditions, W/m^2
i, j, b	power generation equipment, heating equipment, cooling equipment
K_T	temperature coefficient, %/∘C
l	interval length of carbon emissions, kg
L_l	lower heating value of natural gas, kJ/Nm^3
P	electrical power, kW
Q	heating power, kW
r	energy loss coefficient

(*continued on next column*)

(*continued*)

S_{ES}	installed capacity of ES, kW
T	temperature, ∘C
V	natural gas consumption, Nm^3/h
W_K	the cumulative allocated capacity at stage S_K
y	the year within the planning period
Y	planning cycle
Greek symbols	
α	stage
β	price growth rate
β_e	uncompensated carbon emission quotas per unit of electricity, kg/kWh
β_{ea}	values of actual carbon emissions per unit of electricity, kg/kWh
β_h	free carbon emission quota per unit of heat, kg/kWh
β_{ha}	values of actual carbon emissions per unit of heat, kg/kWh
γ	benchmark price, CNY/kg
η	efficiency
λ	unit conversion coefficient, kWh/kJ
μ_{re}	heating -electric ratio of the unit
σ	radiative temperature coefficient
φ	discount rate
$\varphi_{e,h}$	conversion coefficient from the electricity generated by the CHP to the heat generated, kJ/kW
Subscripts/superscript	
c	cost
cha/ds	charging and discharging
C	cooling
gas	natural gas
K	overall planning stage
max/ min	maximum/minimum
n	equipment types
N	number of equipment types
H	heating

Data availability

Data will be made available on request.

Acknowledgements

This work was funded by the Natural Science Foundation of Shandong Province (ZR2021ME199). This work was also supported by the Plan of Introduction and Cultivation for Young Innovative Talents in Colleges and Universities of Shandong Province, and Funding for Domestic Visiting Scholars at Shandong Jianzhu University.

References

[1] J. Guo, D. Wu, Y. Wang, L. Wang, H. Guo, Co-optimization method research and comprehensive benefits analysis of regional integrated energy system, Appl. Energy 340 (2023) 121034, https://doi.org/10.1016/j.apenergy.2023.121034.

[2] J. Ran, Y. Qiu, J. Liu, X. Zhu, J. Liu, Z. Tian, Coordinated optimization design of buildings and regional integrated energy systems based on load prediction in future climate conditions, Appl. Therm. Eng. 241 (2024) 122338, https://doi.org/10.1016/j.applthermaleng.2024.122338.

[3] D. Wu, J. Guo, Optimal design method and benefits research for a regional integrated energy system, Renew. Sustain. Energy Rev. 186 (2023) 113671, https://doi.org/10.1016/j.rser.2023.113671.

[4] A. Alexandria Engineering Journalxuan, S. Tian, A regional integrated energy system load prediction method based on Bayesian optimized long-short term memory neural network, in: Proceedings of the 2021 IEEE PES Innovative Smart Grid Technologies - Asia, ISGT Asia 2021, 2021, https://doi.org/10.1109/ISGTASIA49270.2021.9715617. December 5, 2021 - December 8, 2021, Brisbane, QLD, Australia.

[5] A. Moser, D. Muschick, M. Gölles, P. Nageler, H. Schranzhofer, T. Mach, C. Ribas Tugores, I. Leusbrock, S. Stark, F. Lackner, A. Hofer, A MILP-based modular energy management system for urban multi-energy systems: performance and sensitivity analysis, Appl. Energy 261 (2020) 114342, https://doi.org/10.1016/j.apenergy.2019.114342.

[6] J. Li, D. Li, Y. Zheng, Y. Yao, Y. Tang, Unified modeling of regionally integrated energy system and application to optimization, Int. J. Electr. Power Energy Syst. 134 (2022) 107377, https://doi.org/10.1016/j.ijepes.2021.107377.

[7] T. Liu, D. Zhang, T. Wu, Standardised modelling and optimisation of a system of interconnected energy hubs considering multiple energies—electricity, gas, heating, and cooling, Energy Convers. Manag. 205 (2020) 112410, https://doi.org/10.1016/j.enconman.2019.112410.

[8] J. Wang, H. Deng, X. Qi, Cost-based site and capacity optimization of multi-energy storage system in the regional integrated energy networks, Energy 261 (2022) 125240, https://doi.org/10.1016/j.energy.2022.125240.
[9] J. Sun, J. Xu, D. Ke, S. Liao, Z. Ling, Cluster partition for distributed energy resources in regional integrated energy system, Energy Rep. 9 (2023) 613–619, https://doi.org/10.1016/j.egyr.2023.04.312.
[10] M.G. Prina, M. Lionetti, G. Manzolini, W. Sparber, D. Moser, Transition pathways optimization methodology through EnergyPLAN software for long-term energy planning, Appl. Energy 235 (2019) 356–368, https://doi.org/10.1016/j.apenergy.2018.10.099.
[11] Y. Wang, Y. Wang, Y. Huang, J. Yang, Y. Ma, H. Yu, M. Zeng, F. Zhang, Y. Zhang, Operation optimization of regional integrated energy system based on the modeling of electricity-thermal-natural gas network, Appl. Energy 251 (2019) 113410, https://doi.org/10.1016/j.apenergy.2019.113410.
[12] D. Wu, Z. Han, Z. Liu, P. Li, F. Ma, H. Zhang, Y. Yin, X. Yang, Comparative study of optimization method and optimal operation strategy for multi-scenario integrated energy system, Energy 217 (2021) 119311, https://doi.org/10.1016/j.energy.2020.119311.
[13] Y. Wang, F. Huang, S. Tao, Y. Ma, Y. Ma, L. Liu, F. Dong, Multi-objective planning of regional integrated energy system aiming at exergy efficiency and economy, Appl. Energy 306 (2022) 118120, https://doi.org/10.1016/j.apenergy.2021.118120.
[14] S. Mazzoni, S. Ooi, B. Nastasi, A. Romagnoli, Energy storage technologies as techno-economic parameters for master-planning and optimal dispatch in smart multi energy systems, Appl. Energy 254 (2019) 113682, https://doi.org/10.1016/j.apenergy.2019.113682.
[15] J. Guo, Z. Liu, X. Wu, D. Wu, S. Zhang, X. Yang, H. Ge, P. Zhang, Two-layer co-optimization method for a distributed energy system combining multiple energy storages, Appl. Energy 322 (2022) 119486, https://doi.org/10.1016/j.apenergy.2022.119486.
[16] H.F. Gu, J. Yu, Y.W. Shen, Y. Li, D.J. Guan, P. Ye, Bi-level decentralized optimal economic dispatch for urban regional integrated energy system under carbon emission constraints, IEEE Access 10 (2022) 62341–62364, https://doi.org/10.1109/ACCESS.2022.3177723.
[17] G. Zhu, Y. Gao, Multi-objective optimal scheduling of an integrated energy system under the multi-time scale ladder-type carbon trading mechanism, J. Clean. Prod. 417 (2023) 137922, https://doi.org/10.1016/j.jclepro.2023.137922.
[18] Z. Lyu, Q. Liu, B. Liu, L. Zheng, J. Yi, Y. Lai, Optimal dispatch of regional integrated energy system group including power to gas based on energy hub, Energies 15 (24) (2022), https://doi.org/10.3390/en15249401.
[19] H. Ren, Z. Jiang, Q. Wu, Q. Li, Y. Yang, Integrated optimization of a regional integrated energy system with thermal energy storage considering both resilience and reliability, Energy 261 (2022) 125333, https://doi.org/10.1016/j.energy.2022.125333.
[20] N.E. Koltsaklis, P. Liu, M.C. Georgiadis, An integrated stochastic multi-regional long-term energy planning model incorporating autonomous power systems and demand response, Energy 82 (2015) 865–888, https://doi.org/10.1016/j.energy.2015.01.097.
[21] D. Lei, Z. Zhang, Z. Wang, L. Zhang, W. Liao, Long-term, multi-stage low-carbon planning model of electricity-gas-heat integrated energy system considering ladder-type carbon trading mechanism and CCS, Energy 280 (2023) 128113, https://doi.org/10.1016/j.energy.2023.128113.
[22] X. Lin, N. Zhang, W. Zhong, F. Kong, F. Cong, Regional integrated energy system long-term planning optimization based on multi-energy complementarity quantification, J. Build. Eng. 68 (2023) 106046, https://doi.org/10.1016/j.jobe.2023.106046.
[23] S. Taheri, M. Jooshaki, M. Moeini-Aghtaie, Long-term planning of integrated local energy systems using deep learning algorithms, Int. J. Electr. Power Energy Syst. 129 (2021) 106855, https://doi.org/10.1016/j.ijepes.2021.106855.
[24] Y. Lei, D. Wang, H. Jia, J. Li, J. Chen, J. Li, Z. Yang, Multi-stage stochastic planning of regional integrated energy system based on scenario tree path optimization under long-term multiple uncertainties, Appl. Energy 300 (2021) 117224, https://doi.org/10.1016/j.apenergy.2021.117224.
[25] S. Wang, Y. Qi, K. Xu, D. Ai, L. Zhang, H. Liu, Medium-term and long-term optimal scheduling for community integrated energy system with high proportion of renewable energy and multi-type energy storage, in: Proceedings of the 2022 IEEE International Conference on Power Systems and Electrical Technology, PSET 2022, October 13, 2022 - October 15, 2022, Virtual, Online, Denmark, 2022, https://doi.org/10.1109/PSET56192.2022.10100616.
[26] T.M. Alabi, L. Lu, Z. Yang, Data-driven optimal scheduling of multi-energy system virtual power plant (MEVPP) incorporating carbon capture system (CCS), electric vehicle flexibility, and clean energy marketer (CEM) strategy, Appl. Energy 314 (2022) 118997, https://doi.org/10.1016/j.apenergy.2022.118997.
[27] W. Dong, Z. Lu, L. He, L. Geng, X. Guo, J. Zhang, Low-carbon optimal planning of an integrated energy station considering combined power-to-gas and gas-fired units equipped with carbon capture systems, Int. J. Electr. Power Energy Syst. 138 (2022) 107966, https://doi.org/10.1016/j.ijepes.2022.107966.
[28] Z. Xiong, S. Luo, L. Wang, C. Jiang, S. Zhou, K. Gong, Bi-level optimal low-carbon economic operation of regional integrated energy system in electricity and natural gas markets, Front. Energy Res. 10 (2022) 116436, https://doi.org/10.3389/fenrg.2022.959201.
[29] X. Lyu, T. Liu, X. Liu, C. He, L. Nan, H. Zeng, Low-carbon robust economic dispatch of park-level integrated energy system considering price-based demand response and vehicle-to-grid, Energy 263 (2023) 125739, https://doi.org/10.1016/j.energy.2022.125739.
[30] H. Xiao, F. Long, L. Zeng, W. Zhao, J. Wang, Y. Li, Optimal scheduling of regional integrated energy system considering multiple uncertainties and integrated demand response, Elec. Power Syst. Res. 217 (2023) 109169, https://doi.org/10.1016/j.epsr.2023.109169.
[31] H. Nasrazadani, A. Sedighi, H. Seifi, Enhancing long-term voltage stability of a power system integrated with large-scale photovoltaic plants using a battery energy storage control scheme, Int. J. Electr. Power Energy Syst. 131 (2021) 107059, https://doi.org/10.1016/j.ijepes.2021.107059.
[32] L. Zhang, J. Zhang, P. Ren, L. Ding, W. Hao, C. An, A. Xu, Analysis of energy consumption prediction for office buildings based on GA-BP and BP algorithm, Case Stud. Therm. Eng. 50 (2023) 103445, https://doi.org/10.1016/j.csite.2023.103445.
[33] Y. Gao, Q. Ai, X. He, S. Fan, Coordination for regional integrated energy system through target cascade optimization, Energy 276 (2023) 127606, https://doi.org/10.1016/j.energy.2023.127606.
[34] X. Zong, Y. Yuan, Two-stage robust optimization of regional integrated energy systems considering uncertainties of distributed energy stations, Front. Energy Res. 11 (2023), https://doi.org/10.3389/fenrg.2023.1135056.
[35] B. Jin, Z. Liu, Y. Liao, Exploring the impact of regional integrated energy systems performance by energy storage devices based on a Bi-level dynamic optimization model, Energies 16 (6) (2023), https://doi.org/10.3390/en16062629.
[36] J. Liu, Y. Li, Y. Ma, R. Qin, X. Meng, J. Wu, Two-layer multiple scenario optimization framework for integrated energy system based on optimal energy contribution ratio strategy, Energy 285 (2023) 128673, https://doi.org/10.1016/j.energy.2023.128673.
[37] Y. Li, Z. Liu, Y. Sang, J. Hu, B. Li, X. Zhang, J. Jurasz, W. Zheng, Optimization of integrated energy system for low-carbon community considering the feasibility and application limitation, Appl. Energy 348 (2023) 121528, https://doi.org/10.1016/j.apenergy.2023.121528.
[38] J. Gao, Y. Yang, F. Gao, H. Wu, Two-stage robust economic dispatch of regional integrated energy system considering source-load uncertainty based on carbon neutral vision, Energies 15 (4) (2022), https://doi.org/10.3390/en15041596.
[39] I. Van Beuzekom, B.-M. Hodge, H. Slootweg, Framework for optimization of long-term, multi-period investment planning of integrated urban energy systems, Appl. Energy 292 (2021) 116880, https://doi.org/10.1016/j.apenergy.2021.116880.
[40] G. Zhang, J. Wen, T. Xie, K. Zhang, R. Jia, Bi-layer economic scheduling for integrated energy system based on source-load coordinated carbon reduction, Energy 280 (2023) 128236, https://doi.org/10.1016/j.energy.2023.128236.
[41] R. Wang, L. Yang, X. Wang, Y. Zhou, Low carbon optimal operation of integrated energy system based on concentrating solar power plant and power to hydrogen, Alex. Eng. J. 71 (2023) 39–50, https://doi.org/10.1016/j.aej.2023.03.038.
[42] H. Sun, X. Sun, L. Kou, B. Zhang, X. Zhu, Optimal scheduling of park-level integrated energy system considering ladder-type carbon trading mechanism and flexible load, Energy Rep. 9 (2023) 3417–3430, https://doi.org/10.1016/j.egyr.2023.02.029.
[43] T. Yi, C. Zhang, Scheduling optimization of a wind power-containing power system considering the integrated and flexible carbon capture power plant and P2G equipment under demand response and reward and punishment ladder-type carbon trading, Int. J. Greenh. Gas Control 128 (2023) 103955, https://doi.org/10.1016/j.ijggc.2023.103955.
[44] L. Wang, H. Dong, J. Lin, M. Zeng, Multi-objective optimal scheduling model with IGDT method of integrated energy system considering ladder-type carbon trading mechanism, Int. J. Electr. Power Energy Syst. 143 (2022) 108386, https://doi.org/10.1016/j.ijepes.2022.108386.
[45] F.M. Baba, H. Ge, L. Wang, R. Zmeureanu, Do high energy-efficient buildings increase overheating risk in cold climates? Causes and mitigation measures required under recent and future climates, Build. Environ. 219 (2022) 109230, https://doi.org/10.1016/j.buildenv.2022.109230.
[46] C. Gao, J. Lin, J. Zeng, F. Han, Wind-photovoltaic co-generation prediction and energy scheduling of low-carbon complex regional integrated energy system with hydrogen industry chain based on copula-MILP, Appl. Energy 328 (2022) 120205, https://doi.org/10.1016/j.apenergy.2022.120205.
[47] F. Han, J. Zeng, J. Lin, C. Gao, Multi-stage distributionally robust optimization for hybrid energy storage in regional integrated energy system considering robustness and nonanticipativity, Energy 277 (2023) 127729, https://doi.org/10.1016/j.energy.2023.127729.
[48] J. Ran, J. Ren, J. Liu, B. Gao, A bi-level optimization method for a regional integrated energy system under climate change conditions, in: Proceedings of Building Simulation 2023: 18th Conference of IBPSA, IBPSA, 2023, pp. 2893–2900, https://doi.org/10.26868/25222708.2023.1564.
[49] P. Yang, H. Jiang, C. Liu, L. Kang, C. Wang, Coordinated optimization scheduling operation of integrated energy system considering demand response and carbon trading mechanism, Int. J. Electr. Power Energy Syst. 147 (2023) 108902, https://doi.org/10.1016/j.ijepes.2022.108902.
[50] X. Zhang, S. Chen, Z. Wei, Z. Liang, Low-carbon planning of a park-level integrated energy system considering generalized energy storage, Electr Power Autom Equip. (2023) 1–15, https://doi.org/10.16081/j.epae.202306019.
[51] F. Song, Q. Zhu, R. Wu, Y. Jiang, A. Xiong, B. Wang, Y. Zhu, Q. Li, Meteorological data set for building thermal environment analysis of China, in: Proceedings of Building Simulation 2007: 10th Conference of IBPSA, IBPSA, 2007, pp. 9–16, https://doi.org/10.26868/25222708.2007.920.
[52] P. Li, Z. Wang, H. Liu, J. Wang, T. Guo, Y. Yin, Bi-level optimal configuration strategy of community integrated energy system with coordinated planning and operation, Energy 236 (2021) 121539, https://doi.org/10.1016/j.energy.2021.121539.

[53] X. Hu, H. Zhang, D. Chen, Y. Li, L. Wang, F. Zhang, H. Cheng, Multi-objective planning for integrated energy systems considering both exergy efficiency and economy, Energy 197 (2020) 117155, https://doi.org/10.1016/j.energy.2020.117155.

[54] Q. Lu, W. Zeng, Q. Guo, S. Lü, Optimal operation scheduling of household energy hub: a multi-objective optimization model considering integrated demand response, Energy Rep. 8 (2022) 15173–15188, https://doi.org/10.1016/j.egyr.2022.11.047.

[55] R. Wang, X. Wen, X. Wang, Y. Fu, Y. Zhang, Low carbon optimal operation of integrated energy system based on carbon capture technology, LCA carbon emissions and ladder-type carbon trading, Appl. Energy 311 (2022) 118664, https://doi.org/10.1016/j.apenergy.2022.118664.

[56] Y. Wang, P. Dong, M. Xu, Y. Li, D. Zhou, X. Liu, Research on collaborative operation optimization of multi-energy stations in regional integrated energy system considering joint demand response, Int. J. Electr. Power Energy Syst. 155 (2024) 109507, https://doi.org/10.1016/j.ijepes.2023.109507.

[57] J.W. Gong, Y.P. Li, J. Lv, G.H. Huang, C. Suo, P.P. Gao, Development of an integrated bi-level model for China's multi-regional energy system planning under uncertainty, Appl. Energy 308 (2022) 118299, https://doi.org/10.1016/j.apenergy.2021.118299.

[58] J. Ran, Y. Song, S. Zhou, K. Yang, J. Liu, Z. Tian, A bi-level optimization method for regional integrated energy system considering uncertainty and load prediction under climate change, J. Build. Eng. 84 (2024) 108527, https://doi.org/10.1016/j.jobe.2024.108527.

[59] F. Bu, S. Wang, H. Bai, Y. Wang, L. Yu, H. Liu, An integrated demand response dispatch strategy for low-carbon energy supply park considering electricity–hydrogen–carbon coordination, Energy Rep. 9 (2023) 1092–1101, https://doi.org/10.1016/j.egyr.2023.04.120.

[60] Y. Wang, C. Liu, Y. Qin, Y. Wang, H. Dong, Z. Ma, Y. Lin, Synergistic planning of an integrated energy system containing hydrogen storage with the coupled use of electric-thermal energy, Int. J. Hydrogen Energy 48 (40) (2023) 15154–15178, https://doi.org/10.1016/j.ijhydene.2022.12.334.

[61] C. Gong, Z. Yao, H. Chen, D. Huang, X. Wang, Z. Wang, S. Shi, An optimal coordinated planning strategy for distributed energy station based on characteristics of electric vehicle charging behavior under carbon trading mechanism, Int. J. Electr. Power Energy Syst. 147 (2023) 108884, https://doi.org/10.1016/j.ijepes.2022.108884.

[62] Z. Shi, Y. Yang, Q. Xu, C. Wu, K. Hua, A low-carbon economic dispatch for integrated energy systems with CCUS considering multi-time-scale allocation of carbon allowance, Appl. Energy 351 (2023) 121841, https://doi.org/10.1016/j.apenergy.2023.121841.

[63] S.P. Singh, A.Y. Ku, N. Macdowell, C. Cao, Profitability and the use of flexible CO2 capture and storage (CCS) in the transition to decarbonized electricity systems, Int. J. Greenh. Gas Control 120 (2022) 103767, https://doi.org/10.1016/j.ijggc.2022.103767.

[64] B. Yang, S. Ge, H. Liu, X. Zhang, Z. Xu, S. Wang, X. Huang, Regional integrated energy system reliability and low carbon joint planning considering multiple uncertainties, Sustain Energy Grids 35 (2023) 101123, https://doi.org/10.1016/j.segan.2023.101123.

[65] M. Chen, H. Lu, X. Chang, H. Liao, An optimization on an integrated energy system of combined heat and power, carbon capture system and power to gas by considering flexible load, Energy 273 (2023) 127203, https://doi.org/10.1016/j.energy.2023.127203.

[66] J.H. Zheng, Q.H. Wu, Z.X. Jing, Coordinated scheduling strategy to optimize conflicting benefits for daily operation of integrated electricity and gas networks, Appl. Energy 192 (2017) 370–381, https://doi.org/10.1016/j.apenergy.2016.08.146.